Research Article

Facile synthesis of SiO_2–TiO_2 photocatalyst nanoparticles for degradation of phenolic water pollutants

Khusniddin Musaev[1] · Dilorom Mirkhamitova[1] · Abdurasul Yarbekov[2] · Suvonkul Nurmanov[1] · Khamdam Akbarov[1] · Olim Ruzimuradov[1,2]

Abstract

A facile synthesis of polyethylene glycol-templated silica–titania (PEG-templated SiO_2–TiO_2) nanoparticles has been carried out using sol–gel reactions by partial-prehydrolysis of tetraethoxysilane and titanium isopropoxide. The prepared nanomaterials have been investigated by N_2 adsorption, FTIR, FT-Raman, TG-DSC, XRD, TEM, DLS, ^{13}C and ^{29}Si MAS NMR and XPS analysis to characterize the phase composition and microstructure of the samples. The photocatalytic performance of the SiO_2–TiO_2 nanoparticles was evaluated by photooxidative degradation of the alkylphenol derivatives aqueous solution. It was shown that their photoactivity in the removal of alkylphenol ethoxylates from aqueous solution was higher than for porous titania nanoparticles. The incorporation of PEG template into the inorganic network with subsequent formation of nanoporous structure will increases the efficiency of the SiO_2–TiO_2 nanoparticles. It was shown that the polymeric species played a significant role in the generation of pores by the hybridization with inorganic oxides on the molecular scale due to hydrogen bonds taking place at the ether moieties. The advantages of including thermally removable PEG template in terms of increasing surface, mesoporosity and photon absorbance at UV–visible wavelengths to give nanoengineered photocatalytic materials is described.

Keywords Silica–titania · Nanoparticle · PEG · Phenol derivatives · Photocatalytic activity

1 Introduction

Recently, silica–titania composite materials have been obtained by the sol–gel method and used extensively as the heterogeneous catalysts including silica-supported titania and titanium-substituted mesoporous silica materials [1, 2]. There is a growing interest in the preparation of porous silica–titania materials that have a higher percentage of the titania in a uniformly dispersed state since such materials have some advantages compared to pure titanium oxide [3–5]. It is well known that the reactivity of titanium and silicon alkoxides towards hydrolysis are different [6]. Therefore, the main difficulty in the synthesis of silica–titania consists in providing a good molecular homogeneity. It is necessary to develop a statistical repartition of Si and Ti atoms from the initial reactional mixing, allowing that this process is always preserved in the dried and calcined silica–titania gel. A certain homogeneity in the multi-component inorganic gels requires nearly equal hydrolysis and condensation reaction rates of both reactive species [7].

In the preparation of silica–titania by sol–gel process, controlled hydrolysis is required for obtaining homogeneous gels because reaction rates of hydrolysis and condensation of titanium alkoxides are much higher than those of silicon alkoxides due to the low electronegativity of Ti and its tendency to exhibit multiple coordination states. Consequently, Ti alkoxides have to be stabilized to prevent

✉ Olim Ruzimuradov, o.ruzimuradov@polito.uz; ruzimuradov@rambler.ru | [1]Department of Chemistry, National University of Uzbekistan, Vuzgorodok 15, 100174 Tashkent, Uzbekistan. [2]Department of Natural and Mathematic Sciences, Turin Polytechnic University in Tashkent, Kichik khalqa yoli 17, 100095 Tashkent, Uzbekistan.

SN Applied Sciences (2019) 1:1164 | https://doi.org/10.1007/s42452-019-1192-y

Received: 22 July 2019 / Accepted: 28 August 2019

Published online: 05 September 2019

rapid precipitation, by adding a certain amount of acid into the water-alcohol solution before mixing with the Si alkoxides. A more effective strategy is to introduce a chelating ligand, which can increase the coordination of the metallic center and decrease the reactivity of the precursor molecules [6]. Use of chelating reagent such as acetylacetone and adopting two-step hydrolysis has also been reported to be effective in the improvement of the homogeneity in obtained silica–titania [8]. Nakanishi et al. have reported that the gels with a well-defined micrometer range interconnected macroporous morphology are prepared in silica, titania and silica–titania systems by phase separation [9, 10]. The results suggest that the preparation of silica–titania materials with highly dispersed TiO_2 could also be achieved by extending the sol–gel process. [11].

Phenol and its derivatives are a major source of environmental pollutants. They are considered one of the priority pollutants in wastewater, because they are harmful to organisms even at low concentrations [12]. The phenomena of adsorption from aqueous solution and photocatalytic oxidation of phenolic compounds in heterogeneous photocatalytic system has already been described in several literatures [13, 14]. Mahyar et al. reported that the photocatalytic activity of TiO_2 can be improved by the addition of SiO_2 which increases the available surface area of the catalyst, allowing an increase in adsorption of organic pollutant molecules [15]. Nilchi et al. reported that the sol–gel produced TiO_2/SiO_2 nanoparticle has good photocatalytic properties due to its anatase phase, existence of tetrahedral coordination of TiO_2 in the SiO_2 matrix and very large surface area [16]. Nandanwar et al. studied the synthesis of TiO_2–SiO_2 nanoparticles with using non-ionic surfactants polyethylene glycol (PEG) and polyethylene glycol tert-octylphenyl ether (Triton X-100) at low temperature [17]. They found that Triton X-100 coated TiO_2/SiO_2 sample exhibited higher activity under UV irradiation, due to the low recombination rate of photogenerated electrons and holes. Furthermore, composite photocatalysts have also been tried, such as SiO_2–TiO_2 aerogel studied by Ahmed and Attia [18] and SiO_2–TiO_2 xerogel prepared by Anderson and Bard [19]. It was found that the mixed oxide of SiO_2 and TiO_2 obtained by sol–gel approach was a more efficient photocatalyst for the photodecomposition of organic dyes than pure TiO_2. The presence of an adsorbent (SiO_2) promotes efficiency by increasing the quantity of organic dyes near the TiO_2 sites relative to the solution concentration of dyes [19]. In addition to the better recovery of photocatalyst from the solution, those supports or mixtures were widely reported as good adsorbents for the organics.

In our previous works, the PEG template silica–titania in monolithic and powder forms were prepared by using sol–gel route when the alkoxides are partially pre-hydrolysed or pre-refluxed [8, 20]. Interestingly, the nature of Ti in silica network remains ambiguous. In this work, a facile synthesis of PEG-templated SiO_2–TiO_2 nanoparticles has been carried out using sol–gel reactions by partial-prehydrolysis of tetraethoxysilane and titanium isopropoxide. The present research aimed to explore the nature of Si–O–Ti linkages in nanocomposite xerogels from heterometallic alkoxide precursors to produce better photocatalysts. Photodegradation of phenol and alkylphenol ethoxylates under UV-radiation by PEG-templated SiO_2–TiO_2 composite nanoparticles were measured for evaluating the effects of polymer template on their photocatalytic performances. Nevertheless, there were few research about the investigation of partial-prehydrolysis heterometallic alkoxide precursors.

2 Experimental part

2.1 Materials

Tetraethyl orthosilicate (TEOS) and titanium isopropoxide (TIP) was used as silica and titania sources, respectively. Polyethylene glycol (PEG, m.w. 400, denoted as PEG400) was used as a template. The aqueous solution of 35% hydrochloric acid (HCl) and ammonia (NH_4OH) was used as a catalyst for hydrolysis and polycondensation. All chemicals were obtained from Acros Organics and Sigma-Aldrich Chemie GmbH, Germany and used without further purification.

2.2 Synthesis procedures

The silica sols were produced from the base-catalyzed hydrolysis and condensation of TEOS in ethanol using NH_4OH as the catalyst. The molar concentrations of the pure silica system: 1TEOS:40Ethanol:4Water:0.35NH_4OH. TEOS was added to ethanol and stirred for 5–10 min in a sealed polystyrene container [21]. To this was added deionized water and NH_4OH. The container was then sealed and left for 3 weeks. In the case of polymer/silica preparation, adding them to the TEOS and ethanol mixture before any reaction took place incorporated polymeric species. The solutions were aged at room temperature for 3 weeks. The obtained polymer-templated silica hybrids were dried at 60 °C for 3 days and 100 °C 2 days, dried in a vacuum oven at 120 °C for 1 day, before being separated into smaller samples and calcined at different temperatures (300 °C, 550 °C and 1000 °C) for 3 h in the air to eliminate the polymeric species. All samples before and after calcined were examined by the surface area and structure analysis.

The preparation of polymer-templated titania samples was carried out by using PEG400 as a template and

concentrated HCl was applied as the catalyst. Therefore, HCl, H_2O, and EtOH were added together and stirred for 3–5 min to ensure complete mixing. TIP was added dropwise to the above solution while stirring. The mixture was then prehydrolyzed for ~ 20 min before the PEG template was added. After that, liquid PEG was added directly to the above mixture and the solution was cast into a beaker sealed with paraffin film. This sol solution was then stirred overnight before 10–15 holes were punched in the film to allow the evaporation of volatile molecules such as ethanol and water. The mixture was left at ambient temperature for 2–3 days and then moved to a vacuum oven. It was further dried for another 4–5 days until reaches the constant weight and a transparent and monolithic light yellow disk of PEG containing titania sample was obtained. To remove the template, the as-synthesized samples were ground into fine powders and heat-treated at 300–550 °C. Typical molar composition of all the reactants was 1TIP:40EtOH:3H_2O:0.01HCl.

In the preparation of polymer-templated silica–titania samples, tetraethylorthosilicate in ethanol was hydrolyzed with water that contained 3.6 wt% HCl at room temperature for 30 min; the molar ratios of ethanol and water to tetraethylorthosilicate were 5:1 and 4:1, respectively. Then, the hydrolyzed solution was mixed with titanium isopropoxide that was diluted with ethanol and stirred continuously for 30 min. The molar ratio of ethanol to titanium isopropoxide was 20:1. Finally, an organic polymer (PEG) was added to the solution to control the porosity and the resultant solution was used for future process (coating, powder, etc.). The weight ratio of PEG that was added to the SiO_2–TiO_2 compound was unity [20].

2.3 Characterization

The textural characterization (N_2 adsorption/desorption isotherms) of the powdered samples before and after removing the PEG template was achieved on a Micromeritics ASAP 2010 surface area and pore size analyzer (Micromeritics) at − 196 °C (liquid nitrogen). The samples were degassed at 120 °C overnight before N_2 adsorption–desorption measurement. The surface and pore parameters were calculated using the accompanying software from Micromeritics, Inc. Thermogravimetry–differential thermal analysis (TG–DTA) of the polymer-templated SiO_2–TiO_2 samples was performed with a simultaneous thermal analyzer Netzsch STA 449C (Netzsch Gerätebau GmbH). The measurement was done between room temperature and 700 °C at a heating rate of 5 °C/min under a steady flow of synthetic air (25 ml/min). The X-ray powder diffraction (XRD) patterns of the samples were identified using a STADI P X-ray diffractometer (STOE&Cie GmbH, Germany) with Mo Kα radiation. Transmission electron microscopy (TEM) images for the porous samples were obtained on a Philips CV 200 microscope with an accelerating voltage of 200 keV. Solid-state cross-polarization magic angle spinning nuclear magnetic resonance (CPMAS NMR) experiments were performed on a Bruker AV300 spectrometer operating at a frequency of 75.47 MHz for ^{13}C and 59.62 MHz for ^{29}Si. Dynamic light scattering (DLS) analysis and the ξ (zeta) potential of the polymer-templated silica–titania particles were carried out on a Zetasizer Nano ZS (Malvern Instruments Ltd., UK) that is zeta and size capable—sizing using the NIBS technology (rather than measuring at 90 °C) at 25 °C. Samples were run without further dilution after filtration through a Millipore 0.22 µM. Samples were measured in glass cuvettes with three series of ten reading each being taken. The values recorded are an overall average of the three averages of each series of ten readings. XPS spectra were collected using a PHI 5000 spectrometer and monochromatic AlKα X-ray source (hν = 1486.6 eV) with the electron escape angle of 45° and a pass energy of 23.5 eV. The diameter of the X-ray illuminated sample's area was 200 µm. The UV–vis absorption spectra of the samples were recorded on a Lambda 900 UV/VIS/NIR spectrometer (Perkin-Elmer GmbH, Germany) in the wavelength range of 250–600 nm.

2.4 Photodegradation experiments

The photodegradation experiments start by charging the photoreactor with a 2.8 l solution of either phenol, NP5EO or TX-100 at a controlled pH. The photoreactor consisted of a 3 L Perspex cylindrical reactor (135 mm × 280 mm) with a 400 W medium pressure mercury discharge lamp (Applied Photophysics) at the center of the reactor with a Perspex water cooling jacket. Then the photocatalyst or photocatalyst/adsorbent was added to the photoreactor and the mixture was stirred rapidly for 48 h in the dark and at 296 K ± 1 K (temperature maintained using the water cooling jacket) so that the adsorbent and adsorbate could attain equilibrium. The stirrer speed was reduced to 180 rpm, the air bubbler was turned on and 15 min later the Hg lamp was switched on. Sample of 5 ml was taken at intervals for analysis by UV–Vis absorbance, HPLC and GC–MS. Weight of 1.5 g of TiO_2 photocatalyst was used in every experiment. In experiments with both the photocatalyst and an adsorbent were carried out 3.5 g of adsorbent was used. When using a SiO_2–TiO_2 nanocomposite the weight was selected so that the amount of TiO_2 added was 1.5 g.

2.5 HPLC characterization

The HPLC system used for the analysis of the nonylphenol ethoxylates was a Varian ProStar system with a 9010

solvent delivery system, a 9100 autosampler and a 9065 photodiode array UV–visible detector all controlled with a Varian ProStar Workstation. The column used was a Supelcosil LC-Diol 25 cm x 4,6 mm obtained from Sigma-Aldrich, the mobile phases used were: A: hexane, B: dichloromethane (7): methanol (3), with a gradient of A:B = 90:10 to A:B = 65:35 in 10 min. The mobile phase was passed through the column at 1 cm^3 min^{-1} for 10 min. The photodiode array was set to monitor a wavelength of 273 nm.

3 Results and discussion

The synthesis procedure of PEG-templated SiO_2–TiO_2 using NH_4OH and HCl as a catalyst in the presence of low molecular weight PEG as the template was shown in Fig. 1. It was observed that after removing PEG from the polymer/SiO_2, polymer/TiO_2 and polymer/SiO_2–TiO_2 composites by solvent extraction and heat treatment, mesoporous inorganic oxide networks (silica, titania, and silica–titania) were obtained.

The synthesis procedures basically consisted of three major steps:

1. Pre-hydrolysis of the silicon alkoxide in which a suitable adding sequence of the components is desired;
2. Gelation and drying in the presence of PEG template at room temperature;
3. Removal of the template by heat treatment.

In sol–gel process, inorganic precursors with more than two ligands such as silicon or titanium alkoxide can form a nearly linear chain structure when the reactions are carried out using acid catalysts (normally HCl) with a molar ratio of water to the precursor of ca. 2.0. Excess water increases the functionality of polymerization since the formation of lateral M-OH groups with concerning to the main chain allows branching and/or crosslinking reactions. In the case of titanium alkoxides, due to the high reactivity of Ti–OR bonds towards hydrolysis, the presence of chelating agents is necessary to control the degree of hydrolysis and subsequent polymerization reactions [6, 7].

The textural characterization results of nanoporous silica gel and silica–titania before and after the removal of the template are shown in Figs. 2 and 3. All of these diagrams show the type IV isotherm with the H2 hysteresis, which indicates porosity attributed to capillary condensation in the narrow tubular mesopores with an effective diameter of 2–4 nm [21, 22]. All dimensions of H2 hysteresis loop have a similar size, despite the concentration of template and calcination temperatures. All the hysteresis loops have a certain step in the P/P0 ~ 0.8–1.0.

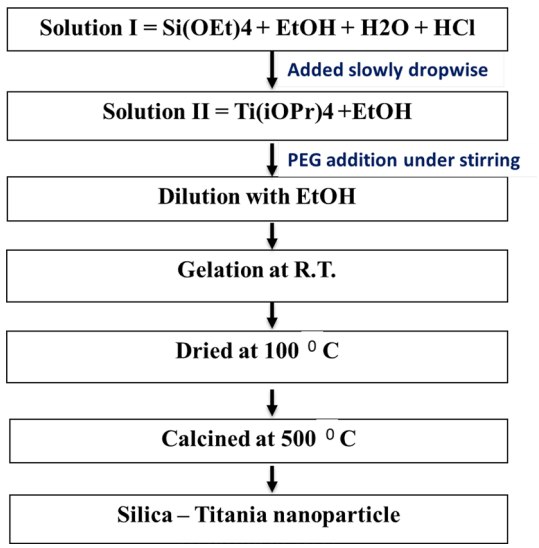

Fig. 1 The general preparation procedure of PEG-templated SiO_2–TiO_2

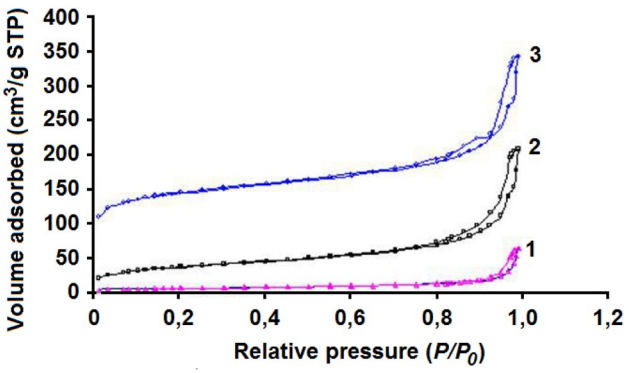

Fig. 2 Nitrogen adsorption–desorption isotherms of silica gel samples before and after removing template at different temperatures: 1—100 °C; 2—550 °C; 3—350 °C

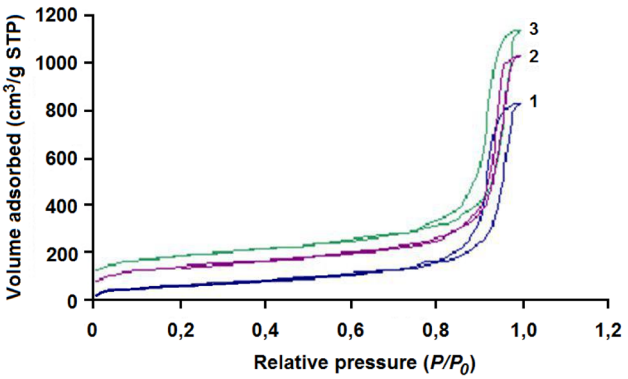

Fig. 3 Nitrogen adsorption–desorption isotherms of silica–titania samples before and after removing template at different temperatures: 1—100 °C; 2—550 °C; 3—350 °C

There is a well-defined plateau after loop $P/P_o > 1.0$, assuming the appearance of pore filling by capillary condensation of nitrogen in the structure instead of adsorption in mesopores of interparticle pore structure [23].

The BET specific surface area and volume of micro- or mesopores to vary with the calcination temperature showed that for the silica obtained with the polymeric template was 490 m^2/g and 0.42 cm^3/g, respectively (Table 1). When the polymer was introduced into silica–titania network the surface area and pore volume decreased to 387 m^2/g and 0.18 cm^3/g respectively, after heat treatment. These data are considered reasonably high for nanoporous silica–titania materials [14]. Using the method of slope of linear regression through the data points suggested in [24–26], it is worth remarking that for PEG/SiO_2, with an increase in the temperature, S_{BET} increases at the rate of 0.309016393. Meanwhile, for PEG/SiO_2–TiO_2, S_{BET} increases with temperature at the rate of 0.69192459.

Vibrational spectroscopic studies (FT-IR and Raman, not shown) of polymer (PEG) connected with inorganic oxides network via physical and chemical bonding were investigated. Raman spectroscopy has been used to see (1) the state of PEG in solution and (2) if any Me–O–C (Me–Si, Ti) bonds were formed in a polymer and silica and or titania interaction during sol formation. In the case of PEG–silica hybrid materials, a defective v (Si–O–Si) band at ~ 560 cm^{-1} (FT-IR) and ~ 490 cm^{-1} (FT-Raman) appeared and increased with increasing PEG concentration. The intensity of vs (Si–OH) band due to residual surface silanol groups, appeared at ~ 960 cm^{-1} (FT-IR) and ~ 980 cm^{-1} (FT-Raman), decreased with increasing content of PEG. The infrared spectra of both as-synthesized PEG/silica and PEG/titania sample show major absorption band associated with PEG molecules. The symmetrical and asymmetrical –CH_2 stretching occur at 2852 and 2922 cm^{-1} respectively; a not very sharp peak at ~ 940 cm^{-1} assigned to Ti–OH species produced from incomplete condensation; the C–C–O stretching vibration designated at ~ 1100 cm^{-1}. It can be clearly noticed that these peaks disappear after heat treatment, indicating complete removal of the PEG template. The only major peak left is the Ti–O stretching vibration at 580 cm^{-1} (not shown).

Using thermal analysis techniques (TG-DSC) it was found that the glass transition temperatures (Tg) (around 348 K and 373 K) of PEG homogeneously embedded in a silica and silica–titania network, respectively, is much higher than that (about 223 K) of pure PEG. The DSC results indicate that the morphology of PEG chains in silica and silica–titania networks changes a lot with the increase in polymer content, from intimately mixing with the silica network to microphase separation, and finally to macrophase separation. When hybrid materials were subjected to thermogravimetric analysis, two weight losses were found in all samples (see Fig. 4). At the lowest temperature (around 373 K), the weight loss corresponds to the removal of physically trapped water and solvents. The next important weight loss between 473 K and 723 K corresponded to the decomposition of PEG and any alkoxide groups (–OR) that remained unreacted during the Si and Ti-alkoxide's hydrolysis and condensation processes.

X-ray diffraction (XRD, not shown) analysis showed that silica powders heat-treated above 1000 °C transformed amorphous silica to a crystalline form. The typical amorphous halo at the 2θ value of 22.5° identifies the amorphous nature of the mesoporous silica heated at around 500 °C, when the temperature goes up to 1200 °C, the amorphous silica transforms into cristobalite. X-ray diffraction pattern for polymer/titania samples heated above 500 °C, some reflections of the anatase crystalline phase, appear on the pattern, indicating that some anatase nanocrystallites are located in the amorphous titania channel walls. The mixed oxides of different composition were subjected to heat treatment above 500 °C to study the eventual formation of crystalline phases. It was found that the sample with the highest titania content retains its amorphous structure up to temperatures of 900 °C with crystallized anatase separated from amorphous silica. The fact that no crystallization is observed can be attributed to the presence of large Si–O–Ti connectivity in the network, and then titania domains are probably too small to crystallize and to be detected [27].

Figure 5 shows the transmission electron microscopy (TEM) image of the PEG-templated silica–titania nanoparticles. The comparison of the pictures shows that TiO_2 and SiO_2 particles surface was surrounded by the polymer

Table 1 Pore parameters of SiO_2 and SiO_2–TiO_2 before and after removing template PEG at different temperatures

Sample	T, °C	S_{BET} ($m^2\ g^{-1}$)	$V_{пор}$ ($cm^3\ g^{-1}$)	D_{BJH} (nm)	D_{BET} (nm)
PEG/SiO_2	100	22	0.049	19	9
PEG/SiO_2	350	490	0.42	9	3
PEG/SiO_2	550	131	0.22	12	7
PEG/SiO_2–TiO_2	100	0.09	0.0007	84	–
PEG/SiO_2–TiO_2	350	387	0.18	3	2
PEG/SiO_2–TiO_2	550	295	0.14	4	2

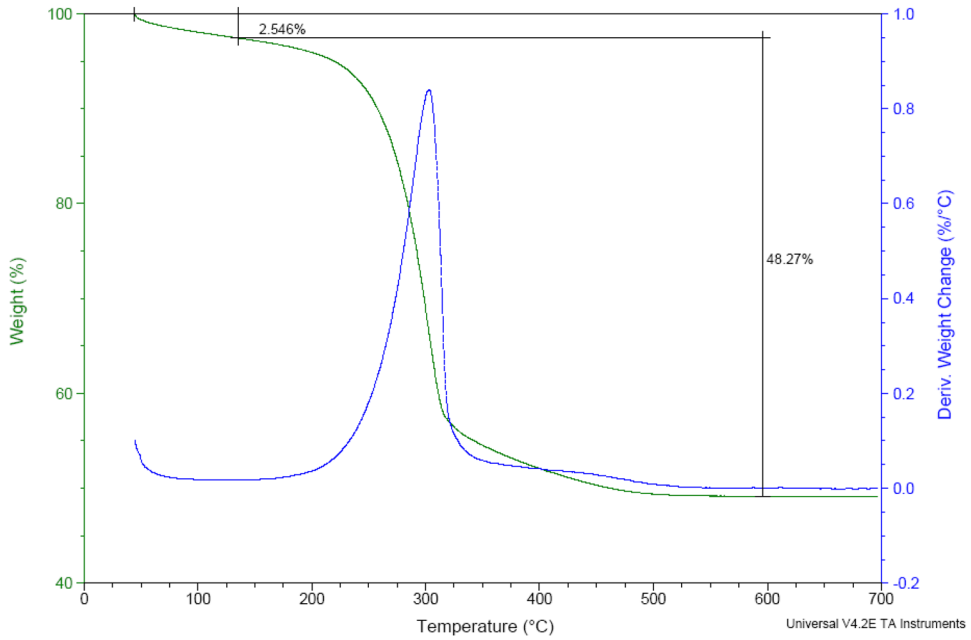

Fig. 4 Thermogravimetric analysis of PEG-templated SiO_2–TiO_2

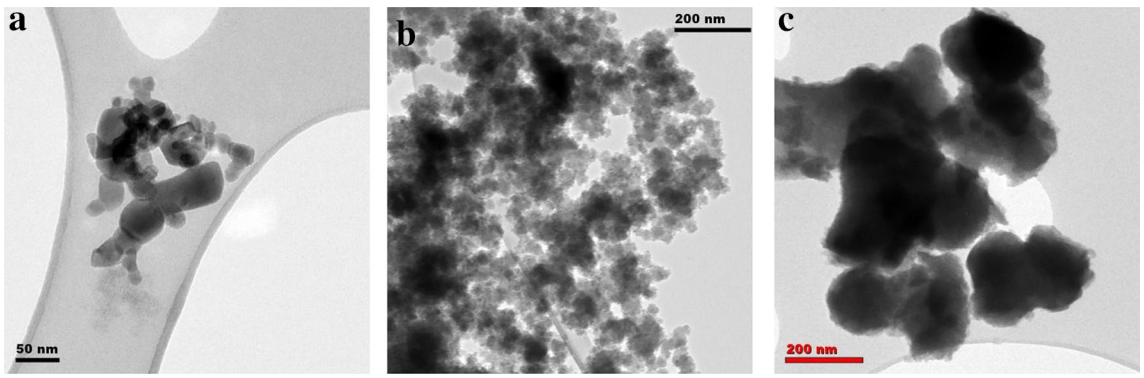

Fig. 5 TEM images of **a** TiO_2, **b** SiO_2 and **c** PEG-templated SiO_2–TiO_2

layer. Micrographs of PEG-templated inorganic oxide networks show that there are have many channels in the material whose diameters are approximately 15–20 nm. Particle aggregates showed nanoporous structures in the micrometer range. It was observed that nano SiO_2 and TiO_2 particles are spherical with an average grain size up to 100 nm.

In Fig. 6, DLS analysis shows that the average diameter of the PEG-templated/silica–titania particles increased up to 100 nm because the former particles include the silica, titania, and polymer, also, there may be the aggregation of nano-silica and titania with sizes about 15–20 nm.

CPMAS NMR experiments were performed on a Bruker AV300 spectrometer operating at a frequency of 75.47 MHz for ^{13}C. The peaks around 62.0 and 70.0 ppm indicated the hydroxyl-bearing carbon and the ether carbon of the polymer (Fig. 7). The peaks at 13.79, 19.16 and 34.87 ppm are characteristic of alkyl units and confirmed the formation of a polymer in an inorganic network [28]. These CPMAS NMR analyses gave more important information about the structure of the polymer/silica, titania and mixed oxide sol–gel materials. The results showed that three states of Si coordination about SiO_4 tetrahedra (Q^2, Q^3, and Q^4) are found with $Q^3 = (SiO)_3Si(OR)$ in the greatest peak [29]. The existence of polymer (PEG) chains has a considerable effect on the structure of the inorganic oxide network. It was shown that the intensity of the methyl resonance peak at 18.0 ppm, which represents the quantity of the Si-ethoxy group, was much smaller than that of the polymer resonance peak around 70.0 ppm as shown in Fig. 7.

XPS analysis of polymer-SiO_2 showed two asymmetric C1s peaks (at 285 and 288 eV) as shown in Fig. 8, alongside O1s at 532.36 eV and Si2p at 102.8 eV. For the polymer-TiO_2

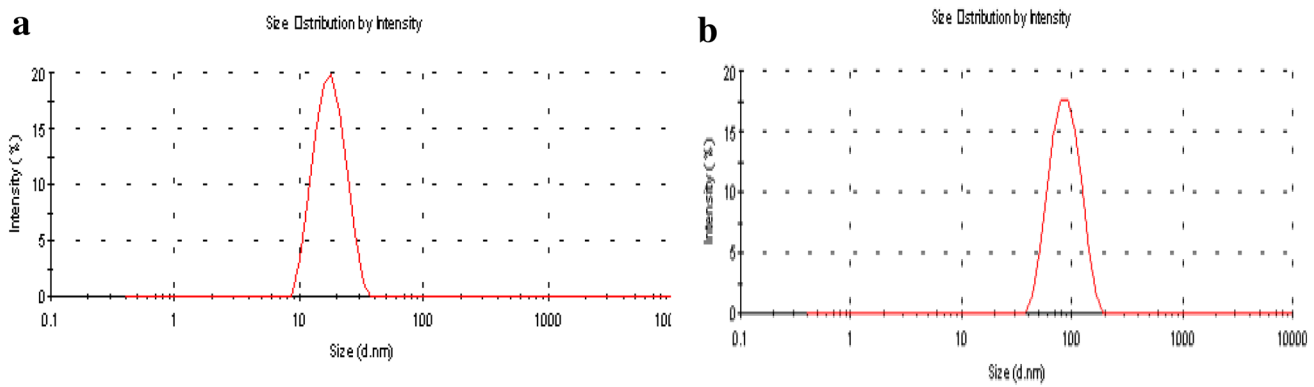

Fig. 6 Particle size distribution seen by DLS for **a** SiO_2 and **b** PEG-templated SiO_2–TiO_2

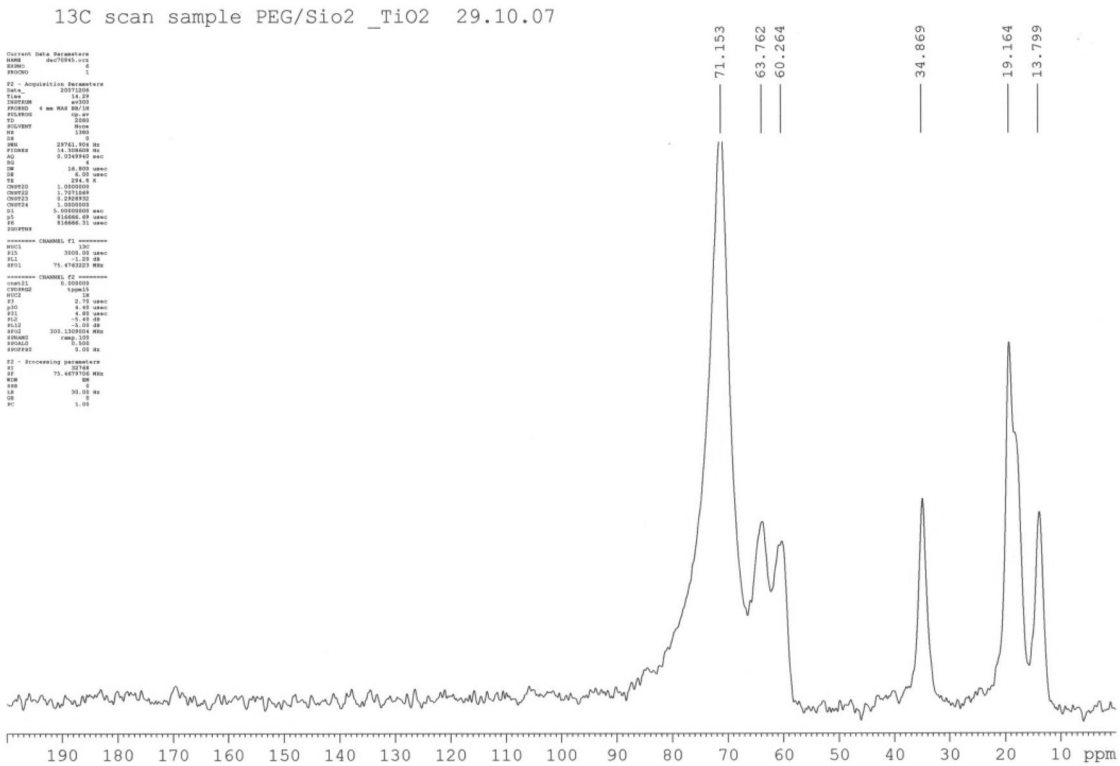

Fig. 7 ^{13}C CPMAS NMR spectra of PEG-templated SiO_2–TiO_2

samples, one C1s (at 285.1 eV) was accompanied by O1s (531.5 eV) and two Ti2p peaks at 457.5 and 463 eV. For polymer-templated silica–titania, there is only one C1 s peak (284 eV), Si2p (101.2 eV), Ti2p (457.62 and 463.7 eV) and O1s (at 529.5 eV (O-Ti) and 531 eV (O-C and O-Si bonds). This downward shift in O1s could be explained by the insertion of Ti^{4+} cations into the tetrahedral sites of the silica network to form Ti–O–Si bonds and the greater electronegativity of Si to that of Ti. From the changes of the chemical shift of O1s peaks, it can be concluded that Ti oxide is combined onto the surface of silica particles through the Ti–O–Si chemical bonding at the interface of the titania and silica particle surface [20].

Initial TiO_2 and PEG-templated SiO_2–TiO_2 nanoparticles have also been studied by diffused reflectance UV spectroscopy. The UV–vis reflectance band edge is a strong function of TiO_2 particle size, which can be attributed to the quantum size effect of semiconductors [30]. Extrapolating the spectral curves to the long-wavelength side provides a measure of the bandgap energy of the

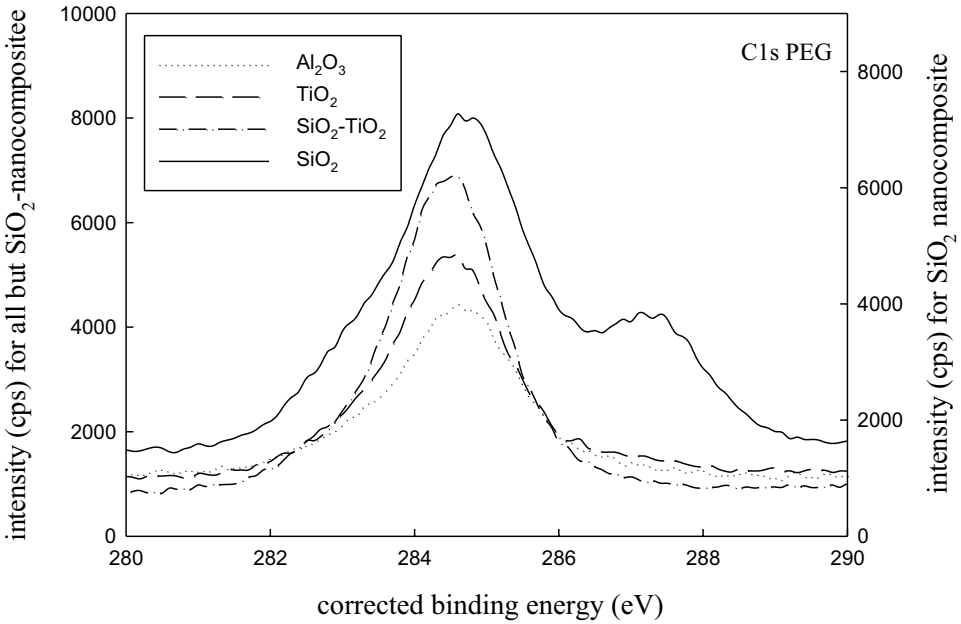

Fig. 8 X-ray photoelectron C1s spectra of PEG-containing nanocomposite sol–gel samples

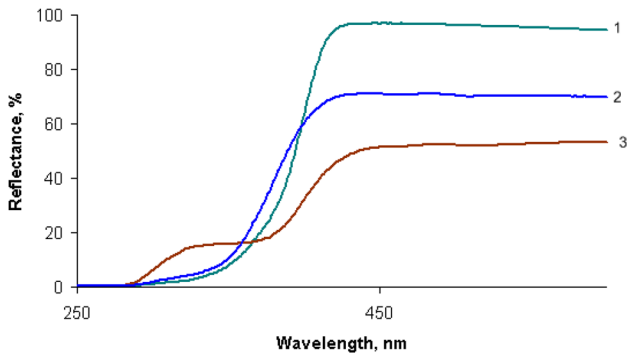

Fig. 9 UV–Vis reflectance spectra of TiO_2-based samples dried at 350 °C. (1) P-25, (2) anatase TiO_2 and (3) PEG-templated SiO_2–TiO_2

nanoparticles. The UV–Vis reflectance of prepared samples as shown in Fig. 9 exhibited an obvious red shift of UV–Vis reflectance spectra of PEG-templated SiO_2–TiO_2 nanoparticles (spectra 3) compared with the spectra of Degussa P-25 (spectrum 1) and anatase TiO_2 nanoparticles (spectrum 2). PEG-templated SiO_2–TiO_2 nanoparticles strongly absorbed UV light within a wavelength above 400 nm, while the non-shape controlled anatase TiO_2 nanoparticles absorbed most of the UV light with a lower wavelength (< 370 nm). This suggests that the polymer-templated SiO_2–TiO_2 nanoparticles have a lower bandgap than the anatase TiO_2 nanoparticles and P25.

The lower bandgap has a positive effect on the photocatalytic activity because lower source energy is needed to arouse a photocatalytic reaction. The redshift of light reflectance of polymer-templated nanoparticles could be due to a large number of surface defects on particle surfaces which make the PEG-templated SiO_2–TiO_2 nanoparticles have a higher ability to capture electron–hole pairs.

The photocatalytic degradation of alkylphenol ethoxylates (APE)—nonyl and octyl-phenol ethoxylates (commercially Igepal CO-520-NPEO and TX-100, respectively) using PEG-templated TiO_2 and SiO_2–TiO_2 has been investigated in detail. The mechanism of the photodegradation of alkylphenol ethoxylates is of great concern. We suggest that the photodegradation initially takes place by cleavage of the ethoxylate chain and shorter chained alkylphenol ethoxylates result. It was also observed agglomeration of the SiO_2 and TiO_2 nanoparticle in suspension during the photodegradation of NPEO and TX-100 and the sedimentation of SiO_2 and TiO_2 nanoparticles on the photooxidation of surfactants.

UV illumination of SiO_2–TiO_2 photocatalyst nanoparticles yields conduction band electrons and valence band holes (Eq. i), which interact with surface adsorbed molecular oxygen to yield superoxide radical anions, $O_2^{-\cdot}$ (Eq. ii), and with water to produce the highly reactive $HO^{\cdot}$ radicals (Eq. iii), respectively. The latter radical species are well known to oxidize a large number of phenolic substrates, for example APE, etc. (Eq. iv).

$$SiO_2 - TiO_2 + h\nu \rightarrow e^-_{cb} + h^+_{vb} \quad \text{(i)}$$

$$e^-_{cb} + O_{2(ads)} \rightarrow O_2^{-\cdot} \quad \text{(ii)}$$

$$h^+_{vb} + Ti{-}OH_2 \rightarrow OH^{\cdot}_{ads} + H^+ \quad \text{(iii)}$$

$$HO^{\cdot} + APE \rightarrow AP + APEO \quad \text{(iv)}$$

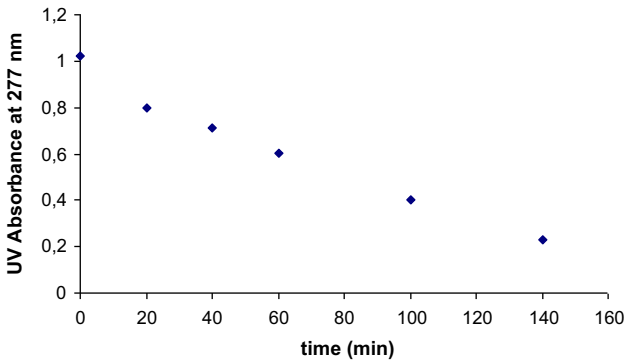

Fig. 10 Photodegradation of TX-100 by PEG-templated SiO_2–TiO_2

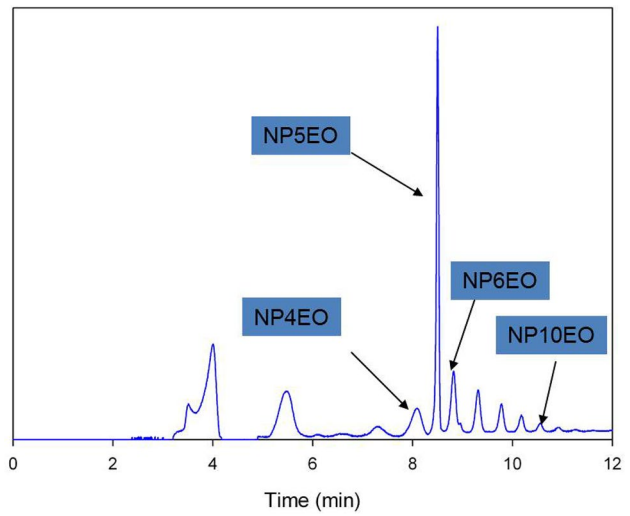

Fig. 11 HPLC of NP5EO solution with UV-irradiated PEG-templated SiO_2–TiO_2 at time = 90 min

Results in Fig. 10 suggest that a bi-product/intermediate was formed in the early stages of the reaction and then it is also photocatalytically degraded. Upon completion of the photocatalytic reaction, the SiO_2 and TiO_2 nanoparticles had aggregated and adhered to the walls of the photoreactor. To determine the reason for this aggregation, the TiO_2 and SiO_2–TiO_2 were removed from the reactor and dried overnight at 348 K. The resulting grey paste was placed in a vial and the amount of solvent (hexane and/or methylene chloride) was added and the vial was shaken for 15 min. The solid was filtered from the solvent and the solvent was removed by N_2 blowdown. The organic residue was re-dissolved in 5 ml of solvent and the sample was analyzed by the HPLC method. The chromatographic analysis shows that several products of photocatalytic degradation have been formed and remain adsorbed on the photocatalyst/adsorbent surface (Fig. 11). It seems to indicate that the removal of the NP5EOs is independent of ethoxylate chain length, i.e. shorter chain ethoxylates are removed at a similar rate to the longer chain ethoxylates. Alkylphenol and APEO with low mass are found in low concentrations in the aqueous solution, which found to be in a high abundance on the surface of the SiO_2 and TiO_2.

There are many opportunities for future study; the sedimentation of the TiO_2 particles is a major problem for the application of photocatalysis in the removal of alkylphenol ethoxylates. The use of stationary support could overcome this problem and ensure that the activity of the TiO_2 remains high even after prolonged use in the photodegradation of these surfactants. Another opportunity for further study arises from a large number of molecules present in the commercial NP5EO, Igepal CO-520, and all the intermediates formed during photodegradation. The use of an NP5EO with only one ethoxylate chain length would enable the identification of photodegradation intermediates and the more accurate measurement of the concentration of the NP5EO used.

Thus, our studies show the incorporation of polymer template into the inorganic network with subsequent formation of nanoporous structure, which increases the efficiency of the sol–gel materials during adsorption/photocatalytic purification and separation of various pollutants of organic origin.

4 Conclusion

In this work, porous silica–titania nanoparticles were synthesized by the hydrolysis and condensation of tetraethyl orthosilicate and titanium isopropoxide in the presence of PEG400 as the pore-forming under careful control of the pH of the solution. It was shown that the polymeric species played a significant role in the generation of pores by the hybridization with inorganic oxides on the molecular scale due to hydrogen bonds taking place at the ether moieties.

Vibrational spectroscopies confirmed the successful incorporation of a polymer in an inorganic network. It was found that the state of PEG in solution and Me–O–C (Me–Si, Ti) bonds were formed in a polymer and silica and/or titania interaction during sol formation. Also, XRD results showed that the silica–titania with the highest titania content retains its amorphous structure up to temperatures of 900 °C. It can be attributed to the presence of large Si–O–Ti connectivity in the network, and then titania domains are probably too small to crystallize in silica network. The average diameter size obtained by TEM and DLS analysis illustrated that because of the aggregation of nanosized silica and titania, the particle size increases up to 100 nm.

It was shown that PEG-templated SiO_2–TiO_2 nanoparticles exhibited higher efficiency in photodegradation of

phenol and alkylphenol ethoxylates under UV than both pure TiO_2 and commercial Degussa P25. During the photodegradation of phenol and APE solutions became discolored, turning brown with the color intensifying as the experiment continued. The photodegradation of APE indicates that a bi-product/intermediate is formed in the early stages of the reaction and then it is also photocatalytically degraded. Upon completion of the photocatalytic reaction, the SiO_2 and TiO_2 nanoparticles had aggregated. The chromatographic analysis shows that several products of photocatalytic degradation had been formed and remains adsorbed on the adsorbent/photocatalyst surface.

Acknowledgements The authors acknowledge the support from the Ministry of Innovation Development of the Republic of Uzbekistan (Projects BF-7-012 and MU-FZ-20171025150). O.R. acknowledges the Erasmus Mundus Chemical Nanoengineering for a Visiting Scholar under which the present study was also carried out.

Compliance with ethical standards

Conflict of interest There is no conflict of interest in the present research.

References

1. Miyazaki S, Miah M, Morisato K, Shintani Y, Kuroha T, Nakanishi K (2005) Titania-coated monolithic silica as separation medium for high performance liquid chromatography of phosphorus-containing compounds. J Sep Sci 28:39
2. Melero JA, Arsuaga JM, De Frutos PG, Iglesias J, Sainz J, Blazquez S (2005) Direct synthesis of titanium-substituted mesostructured materials using non-ionic surfactants and titanocene dichloride. Microporous Mesoporous Mater 86:364
3. Marugan J, Lopez-Munoz M-J, Aguado J, Grieken RV (2007) On the comparison of photocatalysts activity: a novel procedure for the measurement of titania surface in TiO_2/SiO_2 materials. Catal Today 124:103
4. Witte KD, Busuioc AM, Meynen V, Mertens M, Bilba N, Tendeloo GV, Cool P, Vansant EF (2008) Influence of the synthesis parameters of TiO_2–SBA-15 materials on the adsorption and photodegradation of rhodamine-6G. Microporous Mesoporous Mater 110:100
5. Kang C, Jing L, Guo T, Cui H, Zhou J, Fu H (2009) Mesoporous SiO_2-modified nanocrystalline TiO_2 with high anatase thermal stability and large surface area as efficient photocatalyst. J Phys Chem C 113:1006
6. Brinker CJ, Scherer GW (1990) Sol–gel science: the physics and chemistry of sol–gel processing. Academic Press Inc, New York
7. Turova NY, Turevskaya EP, Kessler VG, Yanovskaya MI (2002) The chemistry of metal alkoxides. Kluwer Academic Publishers, Dordrecht
8. Ruzimuradov O, Nurmanov S, Kodani Y, Takahashi R, Yamada I (2012) Morphology and dispersion control of titania–silica monolith with macro–meso pore system. J Sol Gel Sci Technol 64:684
9. Nakanishi K (1997) Pore structure control of silica gels based on phase separation. J Porous Mater 4:67
10. Konishi J, Fujita K, Nakanishi K, Hirao K (2006) Monolithic TiO_2 with controlled multiscale porosity via a template-free sol–gel process accompanied by phase separation. Chem Mater 18:6069
11. Nakanishi K, Motowaki S, Soga N (1992) Preparation of SiO_2–TiO_2 gels with controlled pore structure via sol–gel route. Bull Inst Chem Res Kyoto Univ 70:144–151
12. Lika K, Papadakis IA (2009) Modeling the biodegradation of phenolic compounds by microalgae. J Sea Res 62:135–146
13. McKay G (ed) (1996) Use of adsorbents for the removal of pollutants from wastewaters. CRC Press, Inc., Boca Raton
14. Banerjee G (1997) Treatment of phenolic wastewater in RBC reactor. Water Res 31:705–714
15. Mahyar A, Behnajady MA, Modirshahla N (2010) Characterization and photocatalytic activity of SiO_2–TiO_2 mixed oxide nanoparticles prepared by sol–gel method. Ind J Chem 49:1593–1600
16. Nilchi A, Darzi SJ, Garmarodi SR (2011) Sol–gel preparation of nanoscale TiO_2–SiO_2 composite for eliminating of Con Red Azo Dye. J Mater Sci Appl 2:476–480
17. Nandanwar R, Singh P, Syed F, Haque F (2014) Preparation of TiO_2/SiO_2 nanocomposite with non-ionic surfactants via sol–gel process and their photocatalytic study. Orient J Chem 30:1577–1584
18. Ahmed MS, Attia YA (1995) Aerogel materials for photocatalytic detoxification of cyanide wastes in water. J Non Cryst Solids 186:402–407
19. Anderson C, Bard AJ (1995) An improved photocatalyst of TiO_2/SiO_2 prepared by a sol–gel synthesis. J Phys Chem 99:9882–9885
20. Sermon PA, Leadley JG, MacGibbon RM, Ruzimuradov O (2012) Tuning $X/(TiO_2)_x$–$(SiO_2)_{100-x}$ $(0<x<40)$ xerogel photocatalysts. Ionics 18:455–459
21. Vong MSW, Bazin N, Sermon PA (2004) Chemical modification of silica gels. J Sol Gel Sci Technol 32:293–294
22. Jiao J, Xu Q, Li L (2007) Porous TiO_2/SiO_2 composite prepared using PEG as template direction reagent with assistance of supercritical CO_2. J Colloid Interface Sci 316:596–603
23. Barrett EP, Joyner LS, Halenda PP (1951) The determination of pore volume and area distributions in porous substances. I. Computations from nitrogen isotherms. J Am Chem Soc 73:373–380
24. Animasaun IL, Ibraheem RO, Mahanthesh B, Babatunde HA (2019) A meta-analysis on the effects of haphazard motion of tiny/nano-sized particles on the dynamics and other physical properties of some fluids. Chin J Phys 60:676–687
25. Shah NA, Animasaun IL, Ibraheem RO, Babatunde HA, Sandeep N, Pop I (2018) Scrutinization of the effects of Grashof number on the flow of different fluids driven by convection over various surfaces. J Mol Liq 249:980–999
26. Animasaun IL, Makinde OD, Saleem S (2019) Mixed convection flow of Newtonian fluids over an upper horizontal thermally stratified melting surface of a paraboloid of revolution. J Braz Soc Mech Sci Eng 41:197
27. Ruzimuradov ON (2011) Formation of bimodal porous silica–titania monoliths by sol–gel route. IOP Conf Ser Mater Sci Eng 18:032004
28. Halla JD, Mamak M, Williams DE, Ozin GA (2003) A novel proton conducting solid electrolyte. Adv Funct Mater 13:132–138
29. Chang HY, Thangamuthu R, Lin CW (2004) Structure–property relationships in PEG/SiO_2 based proton conducting hybrid membranes—a 29Si CP/MAS solid-state NMR study. J Membr Sci 228:217–226
30. Monticone S, Tufeu R, Kanaev AV, Scolan E, Sanchez C (2000) Quantum size effect in TiO_2 nanoparticles: does it exist? Appl Surf Sci 162–163:565–570